

Article

The Applicability of TOPSIS- and Fuzzy TOPSIS-Based Taguchi Optimization Approaches in Obtaining Optimal Fiber-Reinforced Concrete Mix Proportions

Mohamed A. Warda¹, Seleem S. E. Ahmad¹, Ibrahim M. Mahdi², Hossam El-Din M. Sallam^{1,*} 
and Hossam S. Khalil¹

¹ Materials Engineering Department, Faculty of Engineering, Zagazig University, Zagazig 44519, Egypt; m.warda22@eng.zu.edu.eg (M.A.W.); ssdawod@eng.zu.edu.eg (S.S.E.A.); hsibrahim@eng.zu.edu.eg (H.S.K.)

² Structural Engineering and Construction Management Department, Future University, Cairo 11835, Egypt; ibrahim.mahdy@fue.edu.eg

* Correspondence: hem_sallam@zu.edu.eg or hem_sallam@yahoo.com

Abstract: This research aims to illustrate and express the impact of analytical techniques such as TOPSIS- and FTOPSIS-based Taguchi models on obtaining the optimum design of fiber-reinforced concrete (FRC). Three levels of silica fume content, fly ash content, water-to-cementitious (W/C) ratio, and superplasticizer content were examined in the present work. However, the steel fiber content (1%) and the maximum aggregate size of 14 mm were kept constant for all mixes. Once the experimental results were obtained following Taguchi's method, it was used as input data to the TOPSIS and FTOPSIS models. The optimum set of mixture factor levels was determined by identifying the two modules. The optimal FRC mix proportions obtained from the TOPSIS- and FTOPSIS-based Taguchi model were 5% silica fume content, 0% fly ash content, 0.27 W/C ratio, and 0.5% superplasticizer. Multi-response optimization approaches are essential to optimize the concrete mix proportions to achieve the required strengths, workability, and production cost. ANOVA was used to analyze the experimental results to find the contribution of each independent variable to the compressive strength and splitting tensile strength of FRC. ANOVA showed that the most predominant factor that affects the FRC mix proportions was the W/C ratio, followed by the fly ash, silica fume, and superplasticizer contents, respectively, in descending order.

Keywords: Taguchi method; TOPSIS; fuzzy TOPSIS; concrete mixture; FRC



Citation: Warda, M.A.; Ahmad, S.S.E.; Mahdi, I.M.; Sallam, H.E.-D.M.; Khalil, H.S. The Applicability of TOPSIS- and Fuzzy TOPSIS-Based Taguchi Optimization Approaches in Obtaining Optimal Fiber-Reinforced Concrete Mix Proportions. *Buildings* **2022**, *12*, 796. <https://doi.org/10.3390/buildings12060796>

Academic Editor: Abdelhafid Khelidj

Received: 19 May 2022

Accepted: 7 June 2022

Published: 9 June 2022

Publisher's Note: MDPI stays neutral with regard to jurisdictional claims in published maps and institutional affiliations.



Copyright: © 2022 by the authors. Licensee MDPI, Basel, Switzerland. This article is an open access article distributed under the terms and conditions of the Creative Commons Attribution (CC BY) license (<https://creativecommons.org/licenses/by/4.0/>).

1. Introduction

There is a wide variety of fibers used in fiber-reinforced concrete (FRC) depending on material, shape, cross-section, and length [1]. Short fibers are commonly added to concrete to increase the toughness and avoid cracking either due to shrinkage during the plastic and drying stages or due to the applied load. The addition of fibers to reinforced concrete elements increased their flexural and shear strengths [2–6]. Recently, matrix-cracked specimens were innovated by Sallam and colleagues to measure the intrinsic fracture toughness of fibrous composite materials [7–11]. Taengua et al. [12] analyzed hundreds of steel fiber-reinforced concrete mixtures compiled from papers published during the last 20 years. They focused on the relationships between the size and dosage of steel fibers and the relative amounts of the constituents of SFRC mixtures.

Most of the optimization methods depending on experiment design have been introduced as one response optimization for researching optimal mix design parameters for concrete. The Taguchi method has been used in optimum conditions for concrete. The advantage of the Taguchi method is keeping the experimental cost at a minimum level. Additionally, it minimizes the variability around the target when the performance value has been brought to the target value. The optimum conditions gained from the experimental

work can also be reproduced in the real production environment, but the Taguchi method considers one response [13–16].

Ye et al. [17] investigated the effect of steel fibers on the mechanical properties of high-strength concrete (HSC). They studied the effect of steel fiber content from 1% to 3%. They found that the best steel fiber content was 2%. On the other hand, Sumathi and Mohan [18] found that the best ratio was 1% for high-strength concrete (HSC). That is why 1% steel fiber was used in the present work to produce fiber-reinforced concrete (FRC). Shokrieh et al. [19] optimized the compressive strength, flexural strength, and interfacial shear strength of polymer concrete using Taguchi orthogonal arrays. Tanyildizi [20] used the Taguchi method to optimize strengthened concrete. Ribeiro et al. [21] used the Taguchi method to analyze the effect of concrete mix proportions and curing on polyester and epoxy concrete flexural strength. Emara et al. [22] investigated the influence of adding rubber to self-compacting concrete and used the Taguchi method as an optimization technique. They considered several concrete mix proportioning constituents.

The fuzzy TOPSIS approach was applied by Ahmed et al. [23] to determine the overall performance of concrete mixing factors and potential order. They found that a concrete mixture with optimum water/cement ratio and high density meets technical, environmental, social, and economic indicators. Zeng et al. [24] demonstrated the application of the Taguchi-based, AHP-weighted TOPSIS method, which helps process engineers select the most optimal process parameter from a large number of conflicting factors for performing electrical discharge machining on ceramics. Karthik and Mohan [25] used the Taguchi method to optimize the mixed proportions of geopolymers to achieve desired strength criteria. They used ANOVA to analyze the experimental results to find the contribution of each independent variable to the compressive strength of the geopolymer concrete.

On the other hand, Ma and colleagues [26–28] used different optimization and reliability techniques to assess rail steel. Furthermore, the Taguchi method has been utilized for various types of concrete [29]. Few types of research involving experimental design include multi-response optimization, such as the technique of ordering preferences by similarity to ideal solutions (TOPSIS) method [29–33]. One of the greatest advantages of the TOPSIS method or fuzzy TOPSIS (FTOPSIS) is not including complex mathematical processes, i.e., it is a simple method [34]. Many types of research incorporate fuzzy logic (FL) into MADM (multi-attribute decision making) [34–39].

This work introduces two models for optimal mixture constituents of FRC. The main contribution of this research is to illustrate the application of the TOPSIS-based Taguchi model and the hybrid FTOPSIS–Taguchi model to expect mixture constituents of FRC. The novelty of the research lies in the comparison of the traditional Taguchi method with the TOPSIS-based Taguchi method and the FTOPSIS-based Taguchi method to obtain the optimal mixture components for FRC.

2. Experimental Work

2.1. Materials

The cement used in this research was SINAI[®] CEM I 52.5N. It has a specific gravity of 3.15. Fly ash class F with a specific gravity of 2.2 was used. Silica fume with a specific gravity of 2.3 was used. Steel fibers were produced by Nassar Group. Their lengths were 24 mm, and their diameters were 0.8 mm. With a density of 1.05 kg/L, a third-generation super plasticizer, Sika ViscoCrete-425, was used for homogeneous concrete in all concrete mixtures. Natural river sand was used as fine aggregates with a specific gravity of 2.6 in the concrete mixtures. The coarse dolomite aggregate had a specific gravity of 2.68 and a maximum size of 14 mm. The ratio between fine and coarse aggregate ranged from 0.37 to 0.39. Figure 1 demonstrates the grading of fine and coarse aggregates.

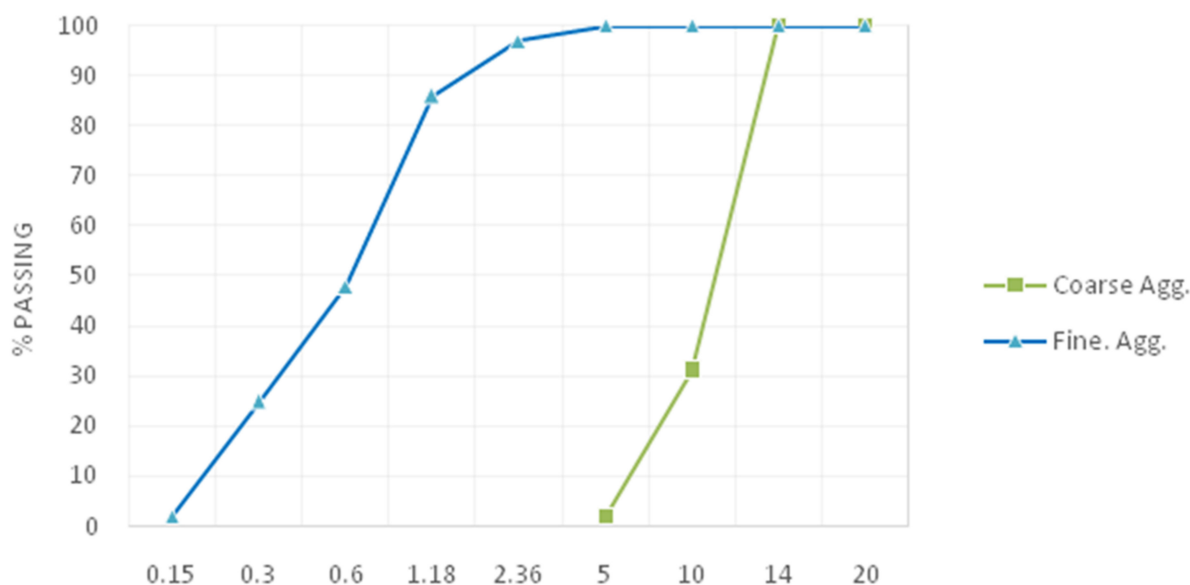


Figure 1. Grading of fine and coarse aggregates. Sieve size, mm.

2.2. Mix Design

Nine FRC mixes were formed. The experiments were designed to give the best possible conditions of the factors influencing the compressive and indirect tensile strengths using Taguchi's orthogonal array. According to FRC properties, 32 to 57 MPa at 28 days compressive strength concrete specimens were produced in this study. Compressive strength at 28 days, splitting tensile strength at 28 days, slump, and the production cost of each mix, were considered. The compressive strength was measured using cubes of 100 mm side-length. The indirect tensile strength was measured by testing cylindrical specimens with 100 mm diameter and 200 mm height. The age of the tested specimens was 28 days. The setup for compressive and indirect tensile tests is shown in Figure 2.

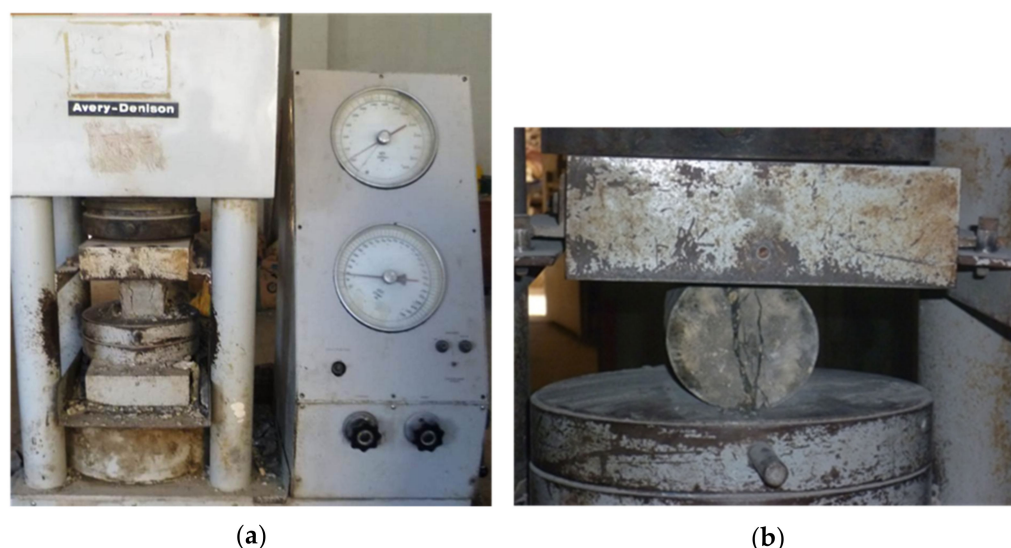


Figure 2. Test setup for (a) compression test and (b) indirect tensile test.

Four factors, i.e., silica fume content (SF), fly ash content (FA), water-to-cementitious (W/C) ratio, and superplasticizer (SP) content, each of which had three levels, as listed in Table 1, were identified as three-level factors. These factors were symbolized as A, B, C, and D, as listed in Table 1. Both SF and FA percentages were used as a partial replacement of the cement content of 550 kg/m³ of the reference mix (Mix No. 1), keeping a total

cementitious content of 550 kg/m³ for all mixes. SP was taken as a percentage of the total cementitious content. The estimated production costs of all nine mixes are listed in Table 2. The orthogonal array and the experimental results are shown in Table 3.

Table 1. Factors and their levels.

| No. | Parameters | Explanation | Levels | | |
|-----|------------|--------------------|-----------|-----------|-----------|
| | | | 1st Level | 2nd Level | 3rd Level |
| 1 | A | Silica fume % | 0 | 5 | 10 |
| 2 | B | Fly ash % | 0 | 10 | 20 |
| 3 | C | W/C ratio | 0.27 | 0.31 | 0.35 |
| 4 | D | Superplasticizer % | 0.5 | 0.7 | 0.9 |

Table 2. Predicted cost for all mixes (LE/m³).

| Mix No. | S. FUME | S. FIBER | SP | Fine Aggregate | Coarse Aggregate | Water | Cement | Fly Ash | Production Cost |
|---------|---------|----------|-------|----------------|------------------|-------|--------|---------|-----------------|
| 1 | 0.0 | 3160.0 | 190.7 | 18.4 | 60.7 | 1.5 | 550.0 | 0.0 | 3981.3 |
| 2 | 0.0 | 3160.0 | 267.2 | 17.5 | 57.8 | 1.7 | 495.0 | 770.0 | 4769.2 |
| 3 | 0.0 | 3160.0 | 342.9 | 16.6 | 55.0 | 1.9 | 440.0 | 1540.0 | 5556.4 |
| 4 | 605.0 | 3160.0 | 342.9 | 17.6 | 58.1 | 1.7 | 522.5 | 0.0 | 4707.8 |
| 5 | 605.0 | 3160.0 | 190.7 | 16.8 | 55.6 | 1.9 | 467.5 | 770.0 | 5267.6 |
| 6 | 605.0 | 3160.0 | 267.2 | 17.8 | 58.9 | 1.5 | 412.5 | 1540.0 | 6062.9 |
| 7 | 1210.0 | 3160.0 | 267.2 | 16.9 | 55.9 | 1.9 | 495.0 | 0.0 | 5206.9 |
| 8 | 1210.0 | 3160.0 | 342.9 | 17.9 | 59.2 | 1.5 | 440.0 | 770.0 | 6001.4 |
| 9 | 1210.0 | 3160.0 | 190.7 | 17.1 | 56.6 | 1.7 | 385.0 | 1540.0 | 6561.2 |

Table 3. Orthogonal array and experimental results.

| MIX No. | S.FUME | FLY ASH | W/C | SP | C28 * | T28 * | S ** | PC *** |
|---------|--------|---------|-----|----|-------|-------|------|-------------------|
| | A | B | C | D | MPa | MPa | mm | LE/m ³ |
| 1 | 1 | 1 | 1 | 1 | 57 | 3.3 | 50 | 3981 |
| 2 | 1 | 2 | 2 | 2 | 39 | 2.3 | 55 | 4769 |
| 3 | 1 | 3 | 3 | 3 | 32 | 1.9 | 50 | 5556 |
| 4 | 2 | 1 | 2 | 3 | 43 | 2.5 | 60 | 4708 |
| 5 | 2 | 2 | 3 | 1 | 40 | 2.4 | 70 | 5268 |
| 6 | 2 | 3 | 1 | 2 | 49 | 2.9 | 50 | 6063 |
| 7 | 3 | 1 | 3 | 2 | 41 | 2.4 | 50 | 5207 |
| 8 | 3 | 2 | 1 | 3 | 56 | 3.3 | 65 | 6001 |
| 9 | 3 | 3 | 2 | 1 | 37 | 2.2 | 50 | 6561 |

* C28 and T28 are compressive and indirect tensile strengths at 28 days, ** S is the slump, and *** PC is the production cost.

3. Multi-Response Optimization Methodology

Figure 3 shows the flow chart illustrating the determination of the optimal mix proportions of the FRC using the fuzzy TOPSIS (FTOPSIS) method. It consists of two phases: experimental design and multi-response optimization module for FRC. The first section includes the determination of FRC performance optimization objectives, as follows:

- Determination of criteria and constraints of mixture proportions, such as compressive strength at 28 days, indirect tensile strength at 28 days, slump, and production cost.
- Determination of factors and their levels include silica fume content, steel fiber content, SP content, W/C ratio, and fly ash content.
- The experiment results were obtained from the first section.

The second section includes a signal-to-noise ratio calculation, the basic concepts of trapezoidal FTOPSIS as shown in Figure 4, determination of the decision matrix,

determination of the fuzzy-weighted normalized decision matrix, identification of a fuzzy positive and negative ideal solution, calculation of separation measures, defuzzification, calculation of similarities to an ideal solution, ranking of reference order, obtaining single response optimization problem, applying Taguchi optimization, and the final determination of optimal factor levels.

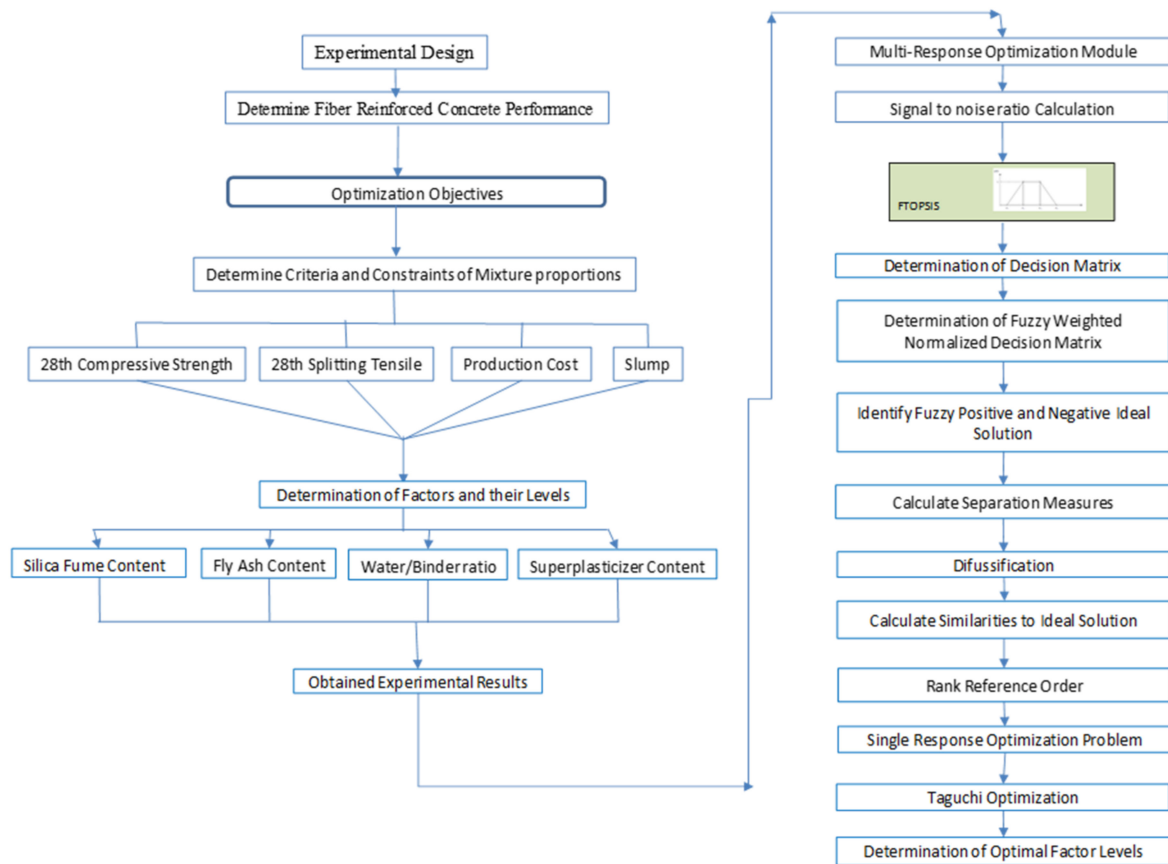


Figure 3. Proposed framework of the fuzzy TOPSIS-based Taguchi model.

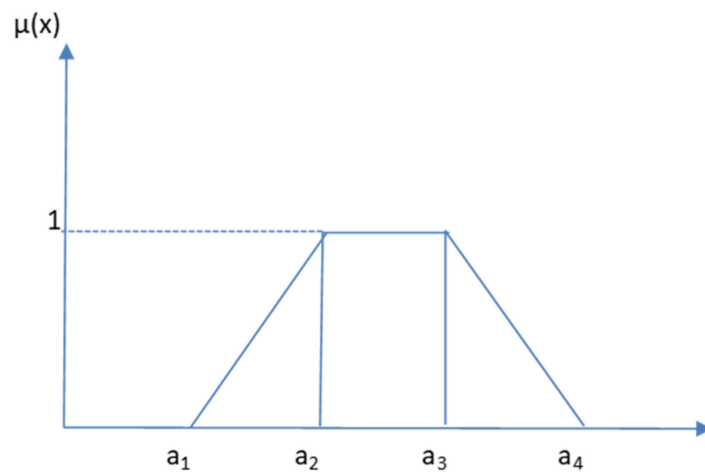


Figure 4. A fuzzy number with a continuous membership function.

The FTOPSIS method incorporates all-determining system performance values into single-column values that can be used as one performance in the multi-response optimization approach. The FTOPSIS-based Taguchi method is easy to apply compared to the other

multi-response optimization methods such as the weighted Grey–Taguchi method and the resolved surface method. The FTOPSIS-based Taguchi method does not need complicated mathematical or statistical equations. The current study compares the results obtained by using the TOPSIS method and the FTOPSIS method. Quality characteristics for the optimization phase of the TOPSIS method are presented in Table 4. Quality characteristics for the optimization phase of the FTOPSIS method are listed in Table 5, where the explanation of trapezoidal fuzzy numbers is shown in Refs. [34,35,39]. Therefore, there are eight quality characteristics identified for HSC. The details of the fuzzy TOPSIS approach are explained elsewhere [34,35,40–47].

Table 4. The weights of each parameter for the TOPSIS method.

| Order | Character | Explanation | Test | Objective | Corresponding Weights * | Normalized Weights |
|-------|-----------|--|------------------------|-------------------|-------------------------|--------------------|
| 1 | C28 | Compressive strength (MPa) 28 days | Hardened concrete test | Larger is better | 9 | 0.36 |
| 2 | T28 | Splitting tensile strength (MPa) 28 days | Hardened concrete test | Larger is better | 3 | 0.12 |
| 3 | S | Slump (mm) | Fresh concrete test | Larger is better | 8 | 0.32 |
| 4 | PC | Production cost (LE/m ³) | Fresh concrete test | Smaller is better | 5 | 0.20 |
| | | Total | | | 25 | 1.0 |

* These values obtained by one expert.

Table 5. The target values of each parameter for FTOPSIS.

| Order | Character | Explanation | Test | Target Values | Weighting of Expert Evaluation (Individual) | | | | Corresponding Fuzzy Weights * | Normalized Fuzzy Weights |
|-------|-----------|--|------------------------|-------------------|---|----------|----------|----------|---|---------------------------|
| | | | | | Expert 1 | Expert 2 | Expert 3 | Expert 4 | | |
| 1 | C28 | Compressive strength (MPa) 28 days | Hardened concrete test | Larger is better | 9 | 8 | 9 | 9 | (8 ^a ,9 ^b ,9 ^c ,9 ^d) | (0.276,0.321,0.321,0.391) |
| 2 | T28 | Splitting tensile strength (MPa) 28 days | Hardened concrete test | Larger is better | 4 | 4 | 3 | 4 | (3,4,4,4) | (0.103,0.143,0.143,0.174) |
| 3 | S | Slump (mm) | Fresh concrete test | Larger is better | 8 | 6 | 8 | 8 | (6,8,8,8) | (0.207,0.286,0.286,0.348) |
| 4 | PC | Production cost (LE/m ³) | Fresh concrete test | Smaller is better | 7 | 6 | 8 | 7 | (6,7,7,8) | (0.207,0.250,0.250,0.348) |
| | | Total | | | | | | | (23,28,28,29) | (0.793,1.0,1.0,1.261) |

* (a,b,c,d) represents a trapezoidal fuzzy number. A trapezoidal fuzzy number (8,9,9,9) [34,35,39].

4. Results and Discussion

4.1. Single-Response Taguchi Optimization

The Taguchi method was conducted through the commercial software Minitab. The greatest probable mix parameter arrangements of the FRC can be found in the main effect plots for the obtained single response. The results of the Taguchi method are (A)₂ (B)₁ (C)₁ (D)₁ for the compressive and indirect tensile strengths as a single response, as shown in Figures 5 and 6, respectively. Additionally, the results of the Taguchi method are (A)₂ (B)₂ (C)₃ (D)₃ for the slump as a single response, as shown in Figure 7.

As the amount of silica fume increased from zero to 5%, an increase in the compressive strength, splitting tensile strength, and workability in terms of the slump values occurred. However, as the percentage of silica fume increased from 5 to 10%, almost no considerable change occurred in the compressive and splitting tensile strengths, while a decrease in the workability was obtained. However, it is known from the literature that this increase in silica fume content as a partial replacement of the cement content results in a further increase in the compressive and splitting tensile strengths of concrete at greater ages, such as at 56 days [48–50]. It is worth recalling that the earlier test age at 28 days can be responsible for this behavior as silica fume reacts with calcium hydroxide, which results from the cement hydration process. On the other hand, a higher amount of silica fume results in less workability as it has a much higher degree of fineness than cement.

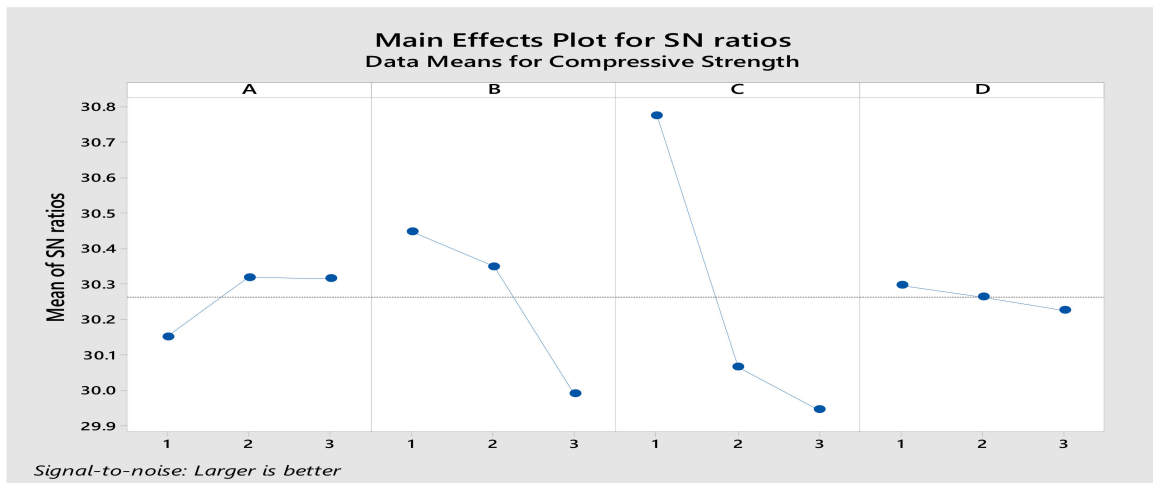


Figure 5. Main effects plot of SN ratios for compressive strength using the Taguchi method.

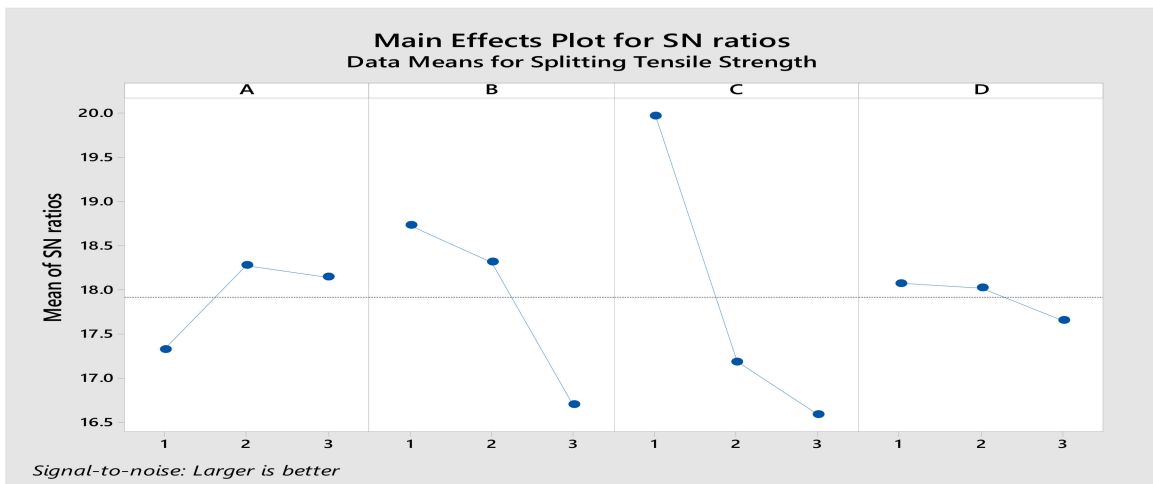


Figure 6. Main effects plot of SN ratios for splitting tensile strength using the Taguchi method.

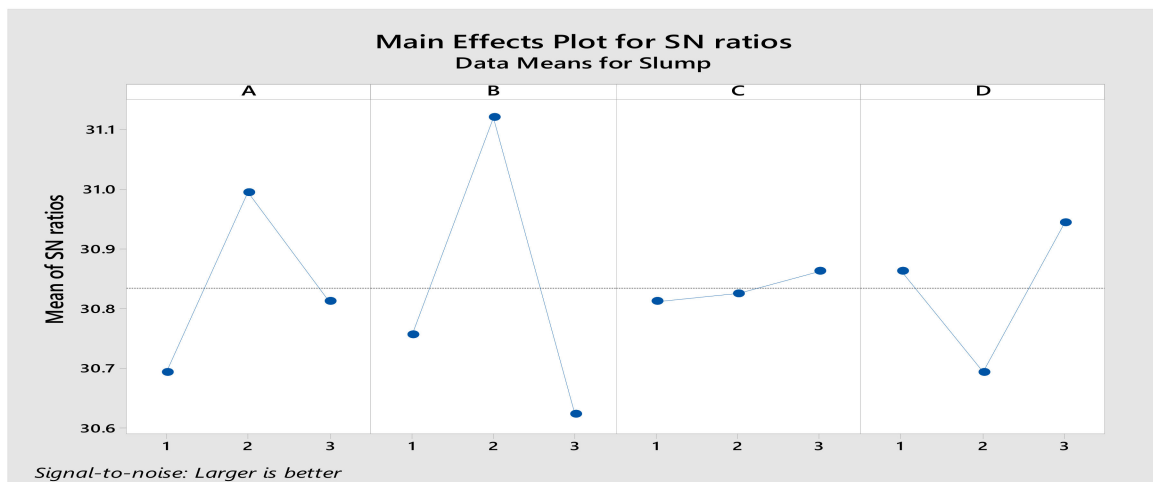


Figure 7. Main effects plot of SN ratios for slump using the Taguchi method.

As the percentage of fly ash increased from zero to 20%, results of the Taguchi analysis showed a decline in the compressive and splitting tensile strengths, as shown in Figures 5 and 6. For the workability in terms of the slump values, the results showed that

adding 10% fly ash as a partial replacement of the cement content improved workability. However, increasing the percentage to 20% led to a decrease in workability.

The reduction in strength may be related to the testing age at 28 days when the fly ash class F used did not yet show its pozzolanic action. However, the opposite trend was observed with the same amount of Portland cement at later ages. This behavior was reported in the literature [51,52]. Figures 5–7 show that the W/C ratio has the most important role in affecting the concrete mixes' compressive strength, splitting tensile strength, and slump values. As the W/C ratio increased, the compressive and indirect tensile strengths decreased while the slump values increased. On the other hand, the increase in the percentage of SP adversely affects the compression and splitting tensile strengths while it increases the concrete slump.

It can be seen from this work and within its limitations that the optimum value of silica fume is the same for the strength and slump of concrete, while the increase of fly ash percentage decreased the concrete strength but improved the concrete slump. Furthermore, the optimum values of W/C ratio and SP content for the concrete strength are opposite to those for the concrete slump. However, it is known from the literature that as SF increases, strength increases, and workability decreases up to a certain limit. In addition, as FA increases, both strength and workability improve up to a certain limit. The test results demonstrated that SF replacement of more than 5% decreased the compressive strength and splitting tensile strength of FRC at 28 days. The reduction is due to their extreme fineness; the water requirement of SF is very high. The water requirement of SF is much higher than the maximum limits stated for FA [14]. Therefore, the reduction in compressive and splitting tensile strengths may be attributed to the fineness of SF. Furthermore, adding SF to the cement matrix may result in micro-shrinkage cracking, which could have a more prominent effect on the strengths.

4.2. Achievement of TOPSIS and FTOPSIS

The greatest probable mix parameter arrangements of FRC can be found in the main effect plots for the single response obtained for the TOPSIS and FTOPSIS methods; see Tables S1–S4 in the Supplementary Materials [29,30,34]. Their related parameter effect plots are shown in Figures 8 and 9. Taguchi's method results led to the final factor design of (A)₂ (B)₁ (C)₁ (D)₁ for the TOPSIS method, see Table 6 and Figure 7. The results of the FTOPSIS method are (A)₂ (B)₁ (C)₁ (D)₁, see Table 7 and Figure 9.

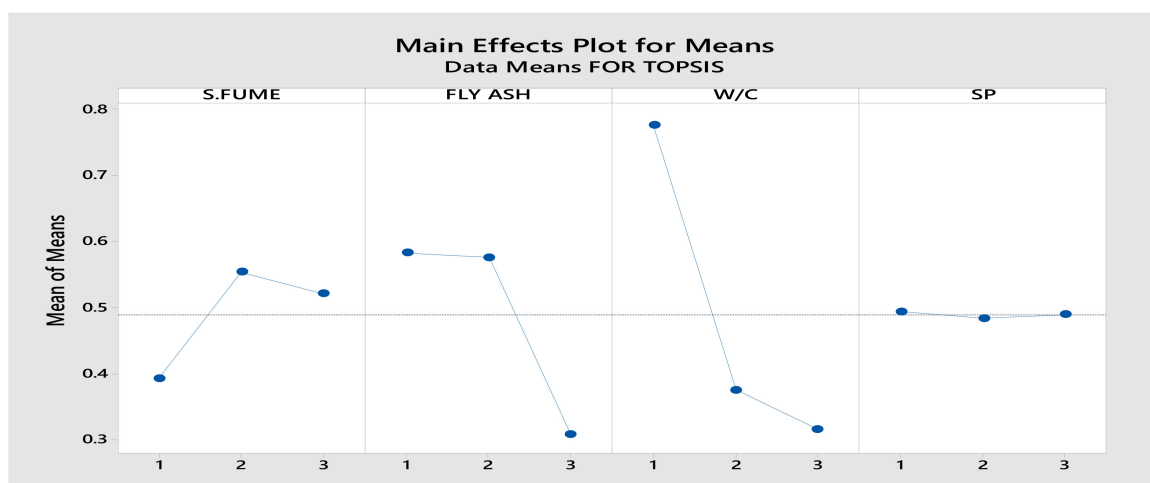


Figure 8. Graphs of parameter effects using TOPSIS.

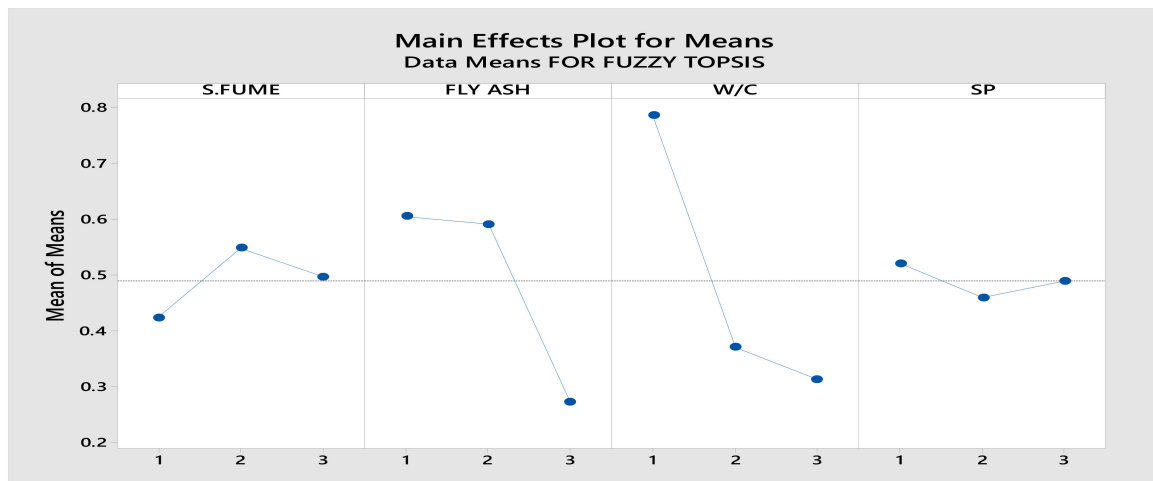


Figure 9. Graphs of parameter effects using FTOPSIS.

Table 6. Optimum factor levels using TOPSIS.

| Factors | SF | FA | W/C Ratio | SP |
|----------------------|--------|--------|-----------|--------|
| Level | A | B | C | D |
| 1 | 0.3921 | 0.5826 | 0.7753 | 0.4935 |
| 2 | 0.5533 | 0.5755 | 0.375 | 0.4835 |
| 3 | 0.5204 | 0.3078 | 0.3155 | 0.4888 |
| Delta | 0.1612 | 0.2748 | 0.4598 | 0.01 |
| Optimal factor level | 2 | 1 | 1 | 1 |

Table 7. Optimum factor levels using FTOPSIS.

| Factors | S. FUME | FLY ASH | W/C m | SP |
|----------------------|---------|---------|--------|--------|
| Level | A | B | C | D |
| 1 | 0.4235 | 0.6051 | 0.7865 | 0.5205 |
| 2 | 0.5485 | 0.5914 | 0.3701 | 0.4591 |
| 3 | 0.4972 | 0.2726 | 0.3125 | 0.4896 |
| Delta | 0.125 | 0.3325 | 0.474 | 0.0614 |
| Optimal factor level | 2 | 1 | 1 | 1 |

It can be seen in Tables 6 and 7 and Figures 8 and 9 that the results of the TOPSIS- and FTOPSIS-based Taguchi approaches are identical. It should be noted that the TOPSIS method results depend on one expert's opinion for the weight of each response; on the other hand, the FTOPSIS method results depend on the opinion of four experts for the weight of each response. Furthermore, the results of TOPSIS and FTOPSIS were identical to the results obtained from Taguchi's single response for compressive and indirect tensile strengths. This may be due to the high weights given to the concrete strengths.

The TOPSIS- and FTOPSIS-based Taguchi methods resulted in 0% fly ash content as the optimum rather than 20% or 10% fly ash content, which means that 0% fly ash content maximizes strengths because the fly ash used was class F (see Figures 3–14, pp. 64 in Kosmatka [53]). It is evident from previous results and studies that fly ash is useful in massive concrete sections because it helps lower the heat of cement hydration. On the other hand, in small concrete elements at room temperature, fly ash may not be as useful, and that is why in this study the beneficial effect of fly ash did not appear or appeared negatively. The concrete specimens in this study were different from massive concrete. If fly ash is more than required to cover the cement particles, surfaces do not benefit from the water demand. The strength of concrete containing fly ash can be higher or lower

than concrete using Portland cement as the only cementing material. Splitting tensile and flexural strengths are affected similarly to compressive strength [16].

The analysis of variance (ANOVA) for compressive and indirect tensile strengths of the concrete mix at 28 days is given in Tables 8 and 9. It is clear that the most predominant factor that affected these results was the W/C ratio of the mix, followed by the fly ash, silica fume, and superplasticizer, in descending order. The important role of the W/C ratio in affecting the test results is well known and appreciable. The contribution of the fly ash to the test results was affected by its type (F) and the test age (28 days). It is worth noting that when all the fly ash type F quantity has reacted with $\text{Ca}(\text{OH})_2$ to produce the additional cementitious material, a larger strength gain would be expected at 56 days and later. When concrete is fully compacted, its strength is inversely proportional to the W/C ratio [54]. This is identical to the results from the TOPSIS- and FTOPSIS-based Taguchi methods. The present study indicated that the lowest W/C ratio, 0.27, maximized the concrete strength.

Table 8. ANOVA for FRC compressive strength at 28 days.

| Source | DF | Seq SS | Contribution | Adj SS | Adj MS | F-Value | p-Value |
|---------|----|---------|--------------|---------|--------|---------|---------|
| S. FUME | 2 | 0.6631 | 2.90% | 0.6631 | 0.3316 | * | * |
| FLY ASH | 2 | 4.7403 | 20.72% | 4.7403 | 2.3701 | * | * |
| W/Cm | 2 | 17.3926 | 76.01% | 17.3926 | 8.6963 | * | * |
| SP | 2 | 0.0862 | 0.38% | 0.0862 | 0.0431 | * | * |
| Error | 0 | * | * | * | * | | |
| Total | 8 | 22.8822 | 100.00% | | | | |

* Not applicable/available.

Table 9. ANOVA for FRC indirect tensile strength at 28 days.

| Source | DF | Seq SS | Contribution | Adj SS | Adj MS | F-Value | p-Value |
|---------|----|---------|--------------|--------|--------|---------|---------|
| S. FUME | 2 | 0.7015 | 3.04% | 0.7015 | 0.3507 | * | * |
| FLY ASH | 2 | 4.847 | 21.02% | 4.847 | 2.4235 | * | * |
| W/Cm | 2 | 17.4149 | 75.52% | 17.415 | 8.7075 | * | * |
| SP | 2 | 0.0961 | 0.42% | 0.0961 | 0.0481 | * | * |
| Error | 0 | * | * | * | * | | |
| Total | 8 | 23.0595 | 100.00% | | | | |

* Not applicable/available.

Furthermore, the ANOVA indicated that the W/C ratio was the most important factor affecting concrete strength. The superplasticizer effect did not appear much in this study because the W/C ratio was the dominant factor; this is clear from the ANOVA, i.e., Tables 8 and 9. It is worth noting that Ozbay et al. [55] found that the least percentage of fly ash gave the maximum compressive strength. These results are also common in the literature [34,56]. This negative effect can also be interpreted as the cement being severely diluted by fly ash and delayed hydration action [14].

There is inconsistency in comparing optimal mix proportions of maximization of a slump from one side and the compressive strength or splitting strength from the other side. This was the reason for applying the multi-response optimization in the present work. There should be approximately the same proportions of the mixture to meet the best of these characteristics. This meets the maximum expectations for compressive strength, splitting tensile strength, and slump, together with production cost minimization. Therefore, the results obtained from the TOPSIS and FTOPSIS models are considered a validation of the results from the Taguchi method.

5. Conclusions

Based on the results presented, the following conclusions can be drawn:

- (1) The results of the TOPSIS and FTOPSIS were identical to the results obtained from Taguchi's single response for compressive and indirect tensile strengths.

- (2) The results from the two models to optimize the FRC mix proportions were 5% silica fume content, 0.5% superplasticizer, 0.27 W/C ratio, and 0% fly ash content.
- (3) ANOVA showed that the most predominant factor that affects the FRC mix proportions was the W/C ratio, followed by the fly ash, silica fume, and superplasticizer, in descending order.
- (4) The effect of fly ash did not appear or appeared negatively for two reasons: first, the type of fly ash, i.e., type F, and second, the FRC strengths were measured at 28 days, not 56 days.

Supplementary Materials: The following supporting information can be downloaded at: <https://www.mdpi.com/article/10.3390/buildings12060796/s1>, Table S1: The decision matrix (S/N ratios), weighted normalized decision matrix, and single response for the TOPSIS method. Table S2: Calculated (S/N) ratios and normalized decision matrix for FTOPSIS. Table S3: Fuzzy TOPSIS application—weighted normalized decision matrix and defuzzification results. Table S4: Fuzzy TOPSIS results.

Author Contributions: Conceptualization, M.A.W., S.S.E.A., I.M.M., H.E.-D.M.S. and H.S.K.; methodology, M.A.W., H.E.-D.M.S. and H.S.K.; formal analysis, M.A.W. and H.S.K.; investigation, M.A.W. and H.S.K.; data curation, M.A.W.; writing—original draft preparation, M.A.W., H.E.-D.M.S. and S.S.E.A.; supervision, S.S.E.A., I.M.M. and H.S.K.; writing—review and editing, M.A.W., H.E.-D.M.S. and H.S.K. All authors have read and agreed to the published version of the manuscript.

Funding: This research received no external funding.

Informed Consent Statement: Not applicable.

Data Availability Statement: All the data required are reported in this manuscript and Supplementary Materials.

Acknowledgments: M.A. Warda especially thanks the staff at the Materials Laboratory, Zagazig University, Egypt, for their cooperation.

Conflicts of Interest: The authors declare no conflict of interest.

References

1. Naaman, A.E. *Fiber Reinforced Cement and Concrete Composites*, 1st ed.; Techno-Press 3000: Sarasota, FL, USA, 2018; p. 34231.
2. Shaaban, I.G.; Said, M.; Khan, S.U.; Eissa, M.; Elrashidy, K. Experimental and theoretical behaviour of reinforced concrete beams containing hybrid fibres. *Structures* **2021**, *32*, 2143–2160. [[CrossRef](#)]
3. Beshara, F.B.A.; Shaaban, I.G.; Mustafa, T.S. Nominal Flexural Strength of High Strength Fiber Reinforced Concrete Beams. *Arab. J. Sci. Eng.* **2012**, *37*, 291–301. [[CrossRef](#)]
4. Said, M.; Abd El-Azim, A.A.; Ali, M.M.; El-Ghazaly, H.; Shaaban, I.G. Effect of elevated temperature on axially and eccentrically loaded columns containing Polyvinyl Alcohol (PVA) fibers. *Eng. Struct.* **2020**, *204*, 110065. [[CrossRef](#)]
5. Said, M.; Montaser, W.; Elgammal, A.S.; Zahir, A.H.; Shaaban, I.G. Shear Strength of Reinforced Mortar Beams Containing Polyvinyl Alcohol Fibre (PVA). *Int. J. Civ. Eng.* **2021**, *19*, 1155–1178. [[CrossRef](#)]
6. Othman, M.A.; El-Emam, H.M.; Seleem, M.H.; Sallam, H.E.M.; Moawad, M. Flexural behavior of functionally graded concrete beams with different patterns. *Arch. Civ. Mech. Eng.* **2021**, *21*, 169. [[CrossRef](#)]
7. El-Sagheer, I.; Abd-Elhady, A.A.; Sallam, H.E.M.; Naga, S.A.R. An Assessment of ASTM E1922 for Measuring the Translaminar Fracture Toughness of Laminated Polymer Matrix Composite Materials. *Polymers* **2021**, *13*, 3129. [[CrossRef](#)]
8. Elakhras, A.A.; Seleem, M.H.; Sallam, H.E.M. Intrinsic fracture toughness of fiber reinforced and functionally graded concretes: An innovative approach. *Eng. Fract. Mech.* **2021**, *258*, 108098. [[CrossRef](#)]
9. Elakhras, A.A.; Seleem, M.H.; Sallam, H.E.M. Fracture toughness of matrix cracked FRC and FGC beams using equivalent TPFM. *Frat. IntegritàStrutt.* **2022**, *60*, 73–88. [[CrossRef](#)]
10. Elakhras, A.A.; Seleem, M.H.; Sallam, H.E.M. Real Fracture Toughness of FRC and FGC: Size and Boundary Effects. *Arch. Civ. Mech. Eng.* **2022**, *22*, 99. [[CrossRef](#)]
11. Ali, A.Y.F.; El-Emam, H.M.; Seleem, M.H.; Sallam, H.E.M.; Moawad, M. Effect of crack and fiber lengths on mode I fracture toughness of matrix-cracked FRC beams. *Constr. Build. Mater.* **2022**, *341*, 127924. [[CrossRef](#)]
12. Taengua, E.G.; Bakhshi, M.; Ferrara, L. Meta-Analysis of Steel Fiber-Reinforced Concrete Mixtures Leads to Practical Mix Design Methodology. *Materials* **2021**, *14*, 3900. [[CrossRef](#)] [[PubMed](#)]
13. Turkmen, I.; Gul, R.; Celik, C.; Demirboga, R. Determination by the Taguchi method of optimum conditions for mechanical properties of high strength concrete with admixtures of silica fume and blast furnace slag. *Civ. Eng. Environ. Syst.* **2003**, *20*, 105–118. [[CrossRef](#)]

14. Hınıslioglu, S.; Bayrak, O.U. Optimization of Early Flexural Strength of Pavement Concrete with Silica Fume and Fly Ash by the Taguchi Method. *Civ. Eng. Environ. Syst.* **2004**, *21*, 79–90. [[CrossRef](#)]
15. Tan, O.; Zaimoglu, A.S.; Hınıslioglu, S.; Altun, S. Taguchi Approach for Optimization of the bleeding on Cement-based grouts. *Tunn. Undergr. Space Technol.* **2005**, *20*, 167–173. [[CrossRef](#)]
16. Warda, M.; Khalil, H.; Ahmad, S.; Mahdi, I. Optimum Sustainable Mix Proportions of High Strength Concrete by Using Taguchi Method. *Frat. Integrità Strutt.* **2020**, *14*, 211–225. [[CrossRef](#)]
17. Ye, L.; Hai, T.K.; Dong, Z. *Optimization of Compressive Strength and Tensile Strength of Ultra High Strength Concrete*; Hiper Mat Proceedings 2016; Universitat Kassel: Kassel, Germany, 2016.
18. Sumathi, A.; Mohan, K.S.R. Effect of Steel Fiber on Structural Characteristics of High Strength Concrete. *Iran J. Sci. Technol. Trans. Civ. Eng.* **2018**, *43* (Suppl. S1), S117–S130. [[CrossRef](#)]
19. Shokrieh, M.M.; Heidari-Rarani, M.; Shakouri, M.; Kashizadeh, E. Effects of thermal cycles on mechanical properties of an optimized polymer concrete. *Constr. Build. Mater.* **2011**, *25*, 3540–3549. [[CrossRef](#)]
20. Tanyildizi, H.; Sahin, M. Application of Taguchi Method for Optimization of Concrete Strengthened with Polymer after High Temperature. *Constr. Build. Mater.* **2015**, *79*, 97–103. [[CrossRef](#)]
21. Ribeiro, M.C.S.; Tavares, C.M.L.; Fieiredo, M.; Ferreira, A.J.M.; Fernandez, A.A. Bending Characteristics of resin Concretes. *Mater. Res.* **2003**, *6*, 247–254. [[CrossRef](#)]
22. Emará, M.A.; Eid, F.M.; Nasser, A.A.; Safaan, M.A. Prediction of Self-compacting Rubberized Concrete Mechanical and Fresh Properties using Taguchi Method. *J. Civil. Environ. Eng.* **2018**, *8*, 2.
23. Ahmed, M.; Mallick, J.; AlQadhi, S.; Ben Kahla, N. Development of Concrete Mixture Design Process Using MCDM Approach for Sustainable Concrete Quality Management. *Sustainability* **2020**, *12*, 8110. [[CrossRef](#)]
24. Zeng, Y.; Lin, C.; Dai, H.; Lin, Y.C.; Hung, J.C. Multi-Performance Optimization in Electrical Discharge Machining of Al₂O₃ Ceramics Using Taguchi Base AHP Weighted TOPSIS Method. *Processes* **2021**, *9*, 1647. [[CrossRef](#)]
25. Karthik, S.; Mohan, K.S.R. A Taguchi Approach for Optimizing Design Mixture of Geopolymer Concrete Incorporating Fly Ash, Ground Granulated Blast Furnace Slag and Silica Fume. *Crystals* **2021**, *11*, 1279. [[CrossRef](#)]
26. Nejad, R.M.; Sina, N.; Ma, W.; Liu, Z.; Berto, F.; Gholami, A. Optimization of Fatigue Life of Pearlitic Grade 900A Steel based on the Combination of Genetic Algorithm and Artificial Neural Network. *Int. J. Fatigue* **2022**, *162*, 106975. [[CrossRef](#)]
27. Nejad, R.M.; Liu, Z.; Ma, W.; Berto, F. Reliability analysis of fatigue crack growth for rail steel under variable amplitude service loading conditions and wear. *Int. J. Fatigue* **2021**, *152*, 106450. [[CrossRef](#)]
28. Nejad, R.M.; Liu, Z.; Ma, W.; Berto, F. Fatigue reliability assessment of a pearlitic Grade 900A rail steel subjected to multiple cracks. *Eng. Fail. Anal.* **2021**, *128*, 105625. [[CrossRef](#)]
29. Simsek, B.; Uygunoglu, T. Multi-response Optimization of Polymer blended Concrete: A TOPSIS based Taguchi application. *Constr. Build. Mater.* **2016**, *117*, 251–262. [[CrossRef](#)]
30. Simsek, B.; Tansel, Y.; Simsek, E.H. A TOPSIS-based Taguchi Optimization to determine Optimal Mixture Proportions of the High Strength Self-compacting Concrete. *Chemom. Intell. Lab. Syst.* **2013**, *125*, 18–32. [[CrossRef](#)]
31. Su, T.L.; Chen, H.W.; Lu, C.F. Systematic Optimization for the evaluation of the microinjection molding parameters of light guide plate with TOPSIS-based Taguchi Method. *Adv. Polym. Technol.* **2010**, *29*, 54–63. [[CrossRef](#)]
32. Hong, G.B.; Su, T.L. Statistical analysis of experimental parameters in characterization of ultraviolet-resistant polyester fiber using a TOPSIS-Taguchi method. *Iran. Polym. J.* **2012**, *21*, 877–885. [[CrossRef](#)]
33. Lan, T.S. Taguchi optimization of multi objective CNC machining using TOPSIS. *Inf. Technol. J.* **2009**, *8*, 917–922. [[CrossRef](#)]
34. Simsek, B.; Tansellc, Y.; Simsek, E.H. Hybridizing a fuzzy multi-response Taguchi optimization algorithm with artificial neural networks to solve standard ready-mixed concrete optimization problems. *Int. J. Comput. Intell. Syst.* **2016**, *9*, 525–543. [[CrossRef](#)]
35. Ic, Y.T. Development of a credit limit allocation model for banks using an integrated Fuzzy TOPSIS and linear programming. *Expert Syst. Appl.* **2012**, *39*, 5309–5316. [[CrossRef](#)]
36. Tong, L.I.; Su, C.T. Optimizing multi-response problems in the Taguchi method by fuzzy multiple attribute decision making. *Qual. Reliab. Eng. Int.* **1997**, *13*, 25–34. [[CrossRef](#)]
37. Lan, T.S. Fuzzy Taguchi deduction optimization on multi-attribute CNC turning. *Trans. Can. Soc. Mech. Eng.* **2010**, *34*, 3–4. [[CrossRef](#)]
38. Sivapirakasam, S.P.; Mathew, J.; Surianarayanan, M. Multi-attribute decision making for green electrical discharge machining. *Expert Syst. Appl.* **2011**, *38*, 8370–8374. [[CrossRef](#)]
39. Ic, Y.T.; Yurdakul, M. Development of a quick credibility scoring decision support system using fuzzy TOPSIS. *Expert Syst. Appl.* **2010**, *37*, 567–574. [[CrossRef](#)]
40. Chen, S.J.; Hwang, C.L. *Fuzzy Multiple Attribute Decision Making*; Springer: Berlin/Heidelberg, Germany, 1992.
41. Negi, D.S. *Fuzzy Analysis and Optimization*. Ph.D. Thesis, Department of Industrial Engineering, Kansas State University, Manhattan, KS, USA, 1989.
42. Chen, C.T. Extensions of the TOPSIS for group decision-making under fuzzy environment. *Fuzzy Sets Syst.* **2000**, *114*, 1–9. [[CrossRef](#)]
43. Cheng, C.H.; Lin, Y. Evaluating the best main battle tank using fuzzy decision theory with linguistic criteria evaluation. *Eur. J. Oper. Res.* **2002**, *142*, 174–186. [[CrossRef](#)]
44. Sen, P.; Yang, J.B. *Multiple Criteria Decision Support in Engineering Design*; Springer: London, UK, 1998.

45. Roy, R.K. *A Primer on the Taguchi Method*; Society of Manufacturing Engineers: Dearborn, MI, USA, 2010; ISBN 0-87263-864-2.
46. Phadke, M.S. *Quality Engineering Using Robust Design*; PTR Prentice-Hall, Inc.: Hoboken, NJ, USA, 1989; ISBN 0-13-745167-9.
47. Taguchi, G. *Taguchi on Robust Technology Development*; The American Society of Mechanical Engineers: New York, NY, USA, 1993; ISBN 0-7918-0028-8.
48. Newman, J.; Choo, B.S. *Advanced Concrete Technology*; Elsevier Ltd.: Oxford, UK, 2003.
49. Amudhavalli, N.K.; Mathew, J. Effect of Silica Fume on Strength and Durability Parameters of Concrete. *Int. J. Eng. Sci. Emerg. Technol.* **2012**, *3*, 28–35.
50. Panjehpour, M.; Ali, A.A.A.; Demirboga, R. A Review for Characterization of Silica Fume and Its Effects on Concrete Properties. *Int. J. Sustain. Constr. Eng. Technol.* **2011**, *2*, 2.
51. ACI 234R-06; ACI Committee 234, Guide For the Use of Silica Fume in Concrete. ACI Committee: Farmington Hills, MI, USA, 2012.
52. ACI 232.2R-18; ACI Committee 232, Report on the Use of Fly Ash in Concrete. ACI Committee: Farmington Hills, MI, USA, 2018.
53. Kosmatka, S.H.; Kerkhoff, B.; Panarese, W.C. *Design and Control of Concrete Mixtures*; Portland Cement Association: Skokie, IL, USA, 2002; ISBN 0-89312-217-3.
54. Neville, A.M. *Properties of Concrete*, 15th ed.; Essex CM20 2JE; Pearson Education Limited: Harlow, UK, 2011.
55. Ozbay, E.; Oztas, A.; Baykasoglu, A.; Ozbebek, H. Investigating mix proportions of high strength self-compacting concrete by using Taguchi method. *Constr. Build. Mater.* **2009**, *23*, 694–702. [[CrossRef](#)]
56. Pala, M.; Ozbay, E.; Oztas, A.; Yuce, M.I. Appraisal of long term effect of fly ash and silica fume on compressive strength of concrete by neural networks. *Constr. Build Mater* **2007**, *21*, 384–394. [[CrossRef](#)]